Atom Indonesia

Journal homepage: http://aij.batan.go.id

Optimization of Residual Stress of High Temperature Treatment Using Genetic Algorithm and Neural Network

M. Susmikanti*[1], A. Hafid[1] and J.B. Sulistyo[2]

[1]*Center for Nuclear Reactor Technology and Safety, National Nuclear Energy Agency Puspiptek Area, Serpong, Tangerang, 15310 Indonesia*

[2]*Center for Nuclear Facilities Engineering, 15310, National Nuclear Energy Agency Puspiptek Area, Serpong, Tangerang, Indonesia*

ARTICLE INFO

Article history:
Received 04 October 2014
Received in revised form 21 April 2015
Accepted 16 June 2015

Keywords:
Residual Stress
Material SS 316
Optimization
Genetic Algorithm
Multi-point binary
Stochastic sampling

ABSTRACT

In a nuclear industry area, high temperature treatment of materials is a factor which requires special attention. Assessment needs to be conducted on the properties of the materials used, including the strength of the materials. The measurement of material properties under thermal processes may reflect residual stresses. The use of Genetic Algorithm (GA) to determine the optimal residual stress is one way to determine the strength of a material. In residual stress modeling with several parameters, it is sometimes difficult to solve for the optimal value through analytical or numerical calculations. Here, GA is an efficient algorithm which can generate the optimal values, both minima and maxima. The purposes of this research are to obtain the optimization of variable in residual stress models using GA and to predict the center of residual stress distribution, using fuzzy neural network (FNN) while the artificial neural network (ANN) used for modeling. In this work a single-material 316/316L stainless steel bar is modeled. The minimal residual stresses of the material at high temperatures were obtained with GA and analytical calculations. At a temperature of 650^0C, the GA optimal residual stress estimation converged at –711.3689 MPa at a distance of 0.002934 mm from center point, whereas the analytical calculation result at that temperature and position is -975.556 MPa . At a temperature of 850^0C, the GA result was -969.868 MPa at 0.002757 mm from the center point, while with analytical result was -1061.13 MPa. The difference in residual stress between GA and analytical results at a temperature of 650^oC is about 27%, while at 850^oC it is 8.67%. The distribution of residual stress showed a grouping concentrated around a coordinate of (-76; 76) MPa. The residuals stress model is a degree-two polynomial with coefficients of 50.33, -76.54, and -55.2, respectively, with a standard deviation of 7.874.

© 2015 Atom Indonesia. All rights reserved

INTRODUCTION

In general, materials used in nuclear power plants are affected by thermal treatment. It is necessary to know the strength of the materials through residual stress. Some of the required information are the optimal value residual stress base on center of thermal treatment, the center of residual stress distribution, and the model prediction of residual stress distribution.

Basically, the welding residuals stress can be predicted using neural network and fuzzy logic modeling [1]. The residual stress was evaluated in steel plates [2]. The laser welding process parameter for super austenitic stainless steel can be optimized using artificial neural networks and genetic algorithm [3]. Beside that, the effect of welding sequence on residual stress distribution in multipass welded piping branch junction was analyzed [4].

* Corresponding author.
E-mail address: mike@batan.go.id
DOI: http://dx.doi.org/10.17146/aij.2015.415

The simulation with finite element for residual stress induced done to dissimilar welding of P92 steel pipe with weld metal IN625 [5]. After then the residual stress on failure pressure of cylindrical pressure vessels was analysed [6]. The neuro-evolutionary models are used for prediction of weld residual stress [7]. The residual stress distributions in welded stainless steel sections have been investigated [8]. As well as, the welding process simulation model for temperature and residual stress was analysed [9]. FEM are use to predict residual stresses in girth welding joint of layered cylindrical vessels [10]. The residual stress can used for fitness assessment of pipe girth welds [11]. The arc welding process for reduced distortion in welded structure was simulation-based numerical optimization [12]. Finally, microstructure and mechanical characteristics of a laser welded joint in SA508 nuclear pressure vessel steel was compared with produced arc-welding [13].

Here, this work is concerning the optimization of variables of residual stresses in model for bars of a single material of 316/316L stainless steel (SS) under high-temperature treatment. The optimization was performed using genetic algorithms (GA). The 316/316L steel is chosen as it is more corrosion-resistant than the more commonly used 304/304L SS. This optimization was performed through the fitness of residual stress function of single bars. Then the residual stress from analytic calculation will be developed to be the model with artificial neural network (ANN). Afterward, the center of residual stress will be developed with fuzzy neural network (FNN). This value can be used to determine the residual stress center of distribution.

EXPERIMENTAL METHODS

Genetic algorithm

Genetic algorithm (GA) is an algorithm which is widely applied to some optimization problem-solving, both for maximization and minimization problems [3]. Genetic algorithms are starting to be used to model and solve complex physical problems, for which analytical solutions are prohibitively difficult to obtain. This algorithm follows the sciences of genetics and natural selection process. Genetic algorithm can also be used for problem solving and relating to a variable or parameter whose value lies within a certain range. In addition, genetic algorithm can be used for problems which have certain restrictions or constraints. This algorithm is usable for finding the solution of general mathematical equation systems, including systems which are impossible, or difficult, to solve analytically [3].

In genetic algorithm, the members of the population of the settlement are called individual samples. In completing the optimization, the algorithm continually searches for a better solution. In every solution, every prospective individual chromosome has properties that can mutate and change. In the simplest solution, the initial solution is repress ented by binary numbers such as 0 and 1 or by real numbers. The evolution starts from a population consisting of a generation of individuals represented by random numbers. The process is repeated. The repetitions are expressed as the next-generation iterations. In every generation, the suitability of each individual in the population is evaluated by a fitness function. The value of the fitness function usually refers to the value of the objective function in optimization problem solving.

The individuals are fitter in the selected population stochastic and each individual is modified in a way which includes crossing back recombination (crossover) and displacement (mutation) at random to form a new generation. The new generation of the chosen solution is then used in the next iteration. The repetition of this procedure is expressed in a set of binary numbers or binary digits in the range of (binary digit/bit) as well as in the ranks of real numbers (the real). The algorithm ends when the maximum number of generations has been produced, or the best approximation level has been reached [3].

There are two types of operators in genetic algorithm, namely the operators to perform recombination, known as recombination or crossover operators, and mutation operators. Recombination operators are subdivided into binary-valued recombination, real-valued recombination, and permutations, whereas mutation operators are subdivided into real-valued mutation and binary-valued mutation. In this work, binary-valued recombination and mutation are selected. The following example shows an initialization procedure for member's generation population in binary digits before recombination:

First chromosome: 1000 | **0100** | **0010**
Second chromosome : 1110 | **0000** | **1000**
After multipoint crossover or recombination, the children chromosomes become:

First chromosome: 1000 | **1000** | **0000**
Second chromosome: 1110 | **0010** | **0100**

A mutation, in genetic algorithm, changes the binary digit (bit) value at a given position. The binary value

1 will be replaced with the binary value 0 and vice-versa. If, for instance, the binary digit in position-9 is 0, after it experiences mutation the binary digit in position-9 becomes 1. Here is an example of a selected chromosome before mutation,

First chromosome: 1110 | 0010 | **0**100

and after mutation,

First chromosome becomes 1110 | 0010 | **1**100

The parameters to be determined in the genetic algorithm include the size of the population declared (*pop size*), the probability of recombination or crossover (*pc*), and the probability of mutation (*pm*). The use of constant values for *pc* and *pm* depends on the size completion of the fitness value. The population size (*popsize*) must be at least 30. The method of selection is a stochastic sampling with replacement. In this method the replacement individuals are probabilistically selected based on their fitness values, starting with the individuals with the largest fitness values; the larger the individual's fitness value, the larger its assigned probability of being selected to reproduce.

A flowchart of the process of genetic algorithm is shown in Fig. 1.

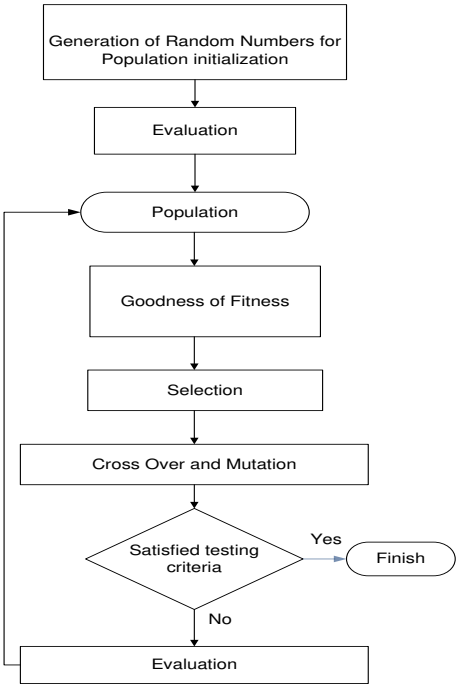

Fig. 1: Flow Diagram of Genetic Algorithms Process.

Artificial neural networks

The artificial neural network (ANN) is a method to allow an object or a system to be trained, such that it will give correct outputs in response to inputs which resemble the input patterns used in training it. The perceptron method is a method for a neural network to learn through observations so that, by using its internal parameters, the network could classify its inputs into recognized categories or classes. A neural network consists of a number of associative neurons and a number of inputs. In designing neural network, specifications have to be given to allow the network to identify its inputs and outputs. For use in pattern recognition applications, the perceptron has to be first prepared, or trained. It has to be coded with a classification matrix containing binary strings representing the classes of inputs. Structurally, the perceptron consists of two stages, or layers, as shown in Fig. 2(a). The first layer of the perceptron assigns weights to the inputs, or in more commonly used terminology, it is a sign detector; it determines the special sign of the input. The second layer of the perceptron is the output layer. It classifies the given data pattern based on the special sign. The learning process makes relevant relationship between weight (b_i) and threshold value (θ). For the problem of classifying to just two classes, the output layer has only one node. Layer 1 continually evaluates weighting functions which take the inputs which are not necessarily binary numbers, and produce outputs in the form of a pattern of binary values x_i of the {0, 1} domain or bipolar values x_i of the {-1, 1} domain. The set of output is element of linear threshold with threshold value following (1),

$$a = f(\sum_{i=0}^{n} b_i p_i + b_0)\,,\; b_0 \equiv -\theta \qquad (1)$$

where b_i represents weights which can be modified due to arrival of signal p_i, and b_o = -(θ) is an approximation to initial values of the weights. Equation (1) indicates that the threshold describe weights as relating the set of output and the arrival signal of shadow x_0 (Fig. 2). The function f(.) is the perceptrons' activation function; here, specifically, it is a tan-sigmoid transfer function following (2),

$$\begin{aligned} \text{step}(x) &= 1 \quad \text{if } x > 0 \\ &= -1 \quad \text{if other} \end{aligned} \qquad (2)$$

The learning procedure takes the weights correlating to the set of output (in the last layer). If the previous weight changes in the last layer only, the use of only one hidden layer in the perceptron in Fig. 2 is justified. The following single-layer perceptron learning algorithm is repeated until convergence is reached. As the first step, select an input vector x from training data. In the second step, if the perceptron gives the wrong answer, modify all weights b_i according to $\Delta b_i = \eta\, a_i p_i$, where a_i is the target of the output and η is the level of learning.

Learning rules can be followed when changing threshold value θ (= $-b_o$) according to equation (1). For example, the architecture of a neural network consisting of neuron *s*, input *r*, and tan-sigmoid transfer function can be expressed in Fig. 2(a) and (b) [1,3];

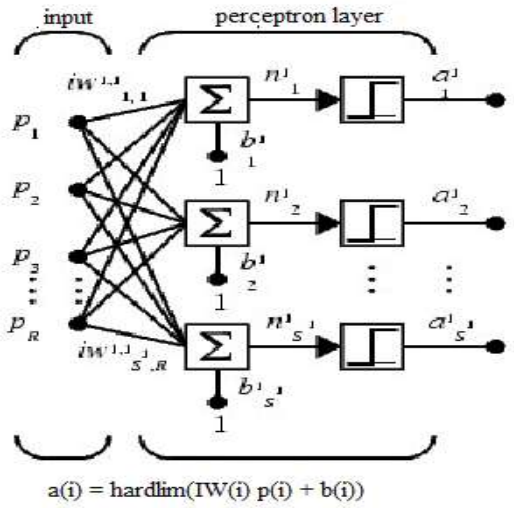

(a)

Fig. 2(a). Architecture of ANN [1].

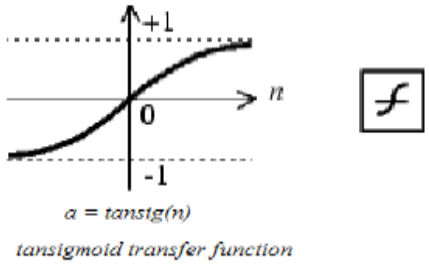

(b)

Fig. 2(b). Tan-Sigmoid Transfer function [1].

Fuzzy neural network

The fuzzy neural network (FNN) is described in (3),

$$F = \exp(-\mu_1 E_1 - \mu_2 E_2 - \mu_3 E_3 - ..... - \mu_k E_k) \quad (3)$$

Where $\mu_1, \mu_2, \mu_3, ..., \mu_k$ are the weighting coefficients and $E_1, E_2, ..., E_k$ have a concept of energy [7,14,15]. The center value parameters are defined in (4),

$$E_i = \sqrt{\frac{1}{N_i}\sum_{i=1}^{N_i}(y_i(k) - y_i(\bar{k}))^2} \quad (4)$$

Residual stress

A simple model [Tim A. Osswald, 1998] for the calculation of residual stress in a bar of a single material is given in (5) [16],

$$\sigma(z) = -\frac{2}{3}\alpha E(T_s - T_f)(\frac{3z^2}{2L^2} - \frac{1}{2}) \quad (5)$$

The residual stress distribution follows a quadratic temperature distribution. We assume no additional residual stresses during the phase change. This function can be used to estimate the distribution of residual stress in thin samples. In this case, the parameter T_f is the final temperature of the part, E is Young's modulus, α is the coefficient of thermal expansion, L is half the thickness, and T_s is the solidification temperature. The unit of residual stress $\sigma(z)$ is MPa and the unit of z is mm. The parameter z is the distance from the center point where the heating process takes place.

RESULTS AND DISCUSSION

In the residual stress equation (5), there are several parameters whose values can be expressed as constants or as values in fixed ranges (thus, restricted to certain intervals). We use the 316/316L SS which is more corrosion-resistant than the more commonly used 304/304L SS. The initial temperature in the solid state T_s is 20°C (room temperature) and the final temperature T_f ranges between 650°C and 1000°C. However, in simulation, T_f is treated as a constant; its value is changed only at the beginning of a simulation run. Likewise, the parameter L shows the average thickness and is between 0.25 mm and 6.35 mm, but is treated as a simulation constant. The constant E indicates the Young's modulus of 200×10^3 MPa.The coefficient of thermal expansion α is expressed with a value of 1.94×10^{-5} at the temperature range of 20°C-1000°C and 1.82×10^{-5} at the temperature range of 20°C - 500°C. The values of z, which is the center point of high temperature treatment, are given in the range of (-5; 5) mm rather than as a constant.

Based on the assumption that the temperature distribution is parabolic [16], the parabolic models can be used to illustrate how the residual stress behaves during high temperature processes. It starts from temperatures T_{f1} and T_{f2} of 100°C and 500°C, respectively, as shown in Fig. 3. The optimization of the genetic algorithm with multiple parameters was performed using the existing facilities and functions in MATLAB.

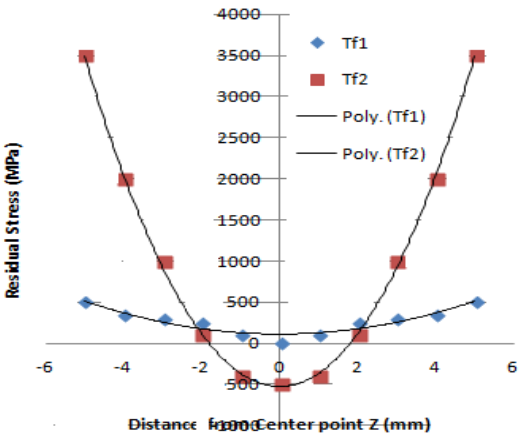

Fig. 3. Residual stress curve during temperature process *Tf1* at 100^{0}C and *Tf2* at 500^{o}C.

Optimization was performed on the residual stress equation which in this case is expressed as a function of genetic algorithm. For the control parameters in the genetic algorithm, the population size (*pop size*) was set constant at the previously stated minimum of 30, while the probability of crossover *(pc)* and the probability of mutation *(pm)* were set at 0.25 and 0.01, respectively. The simulations achieved the objective function of minimal residual stress with the distance *z*. The residual stresses in the simulation iterations performed to reach the 50th generation, with each generation have population size of 30. The optimal value of residual stress was obtained when the fitness of objective function is reached.

The minimal value of the residual stress of the 316/316L SS at a temperature of 650^{o}C converged to or was best at -711.3689 MPa (-711.4 MPa), which is given in Fig. 4 and Table 1. Its position *z* is obtained as 0.002934 mm from the center point for the residual stress of -711.4 MPa.

Table 1. Optimal Residual Stress at 650^{o}C

Number of Generation	Size of Pop.	Best Fitness
1	30	2482
2	60	2482
3	90	2482
4	120	2482
5	150	2482
6	180	2482
7	210	2482
8	240	-967.9
9	270	-967.9
10	300	-967.9
:	:	
45	1350	-969.9
46	1380	-969.9
47	1410	-969.9
48	1440	-969.9
49	1470	-969.9
50	1500	-969.9

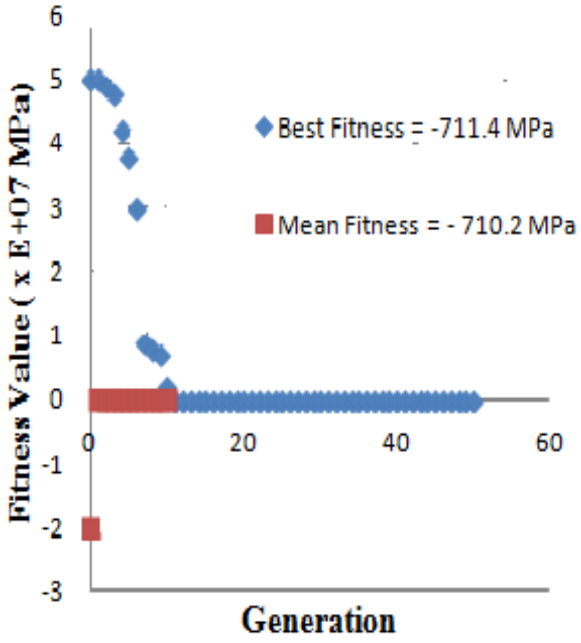

Fig. 4. Optimal residual stress of 316/316L SS at 650^{o}C.

From Table 1, in the last six simulations (from generation-45 to generation-50) the residual stress was stable or convergent at -711.4 MPa. This value is also shown in Fig. 4.

At the temperature of 850^{o}C, the optimal residual stress values converged to -969.868 MPa, which is given in Fig. 5 and Table 2. The position *z* is 0.002757 mm from the center point for the optimal residual stress on-969.868 MPa. In Table 2, the residual stress remains constant from generation-45 until generation-50. The value of residual stress is stable at -969.9 MPa as shown in Fig. 5.

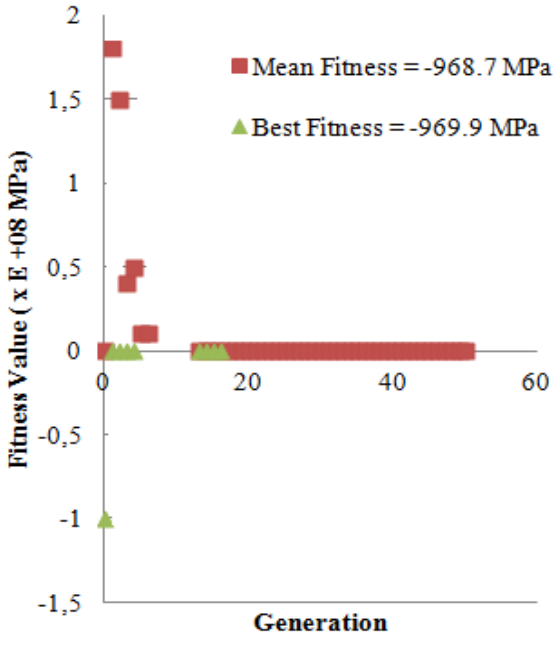

Fig. 5. Optimal residual stress for 316/316L SS at 850^{o}C.

Table 2. Optimal Residual Stress at 850°C

Number of Generation	Size of Pop.	Best Fitness (MPa)
1	30	-688.1
2	60	-688.1
3	90	-688.1
4	120	-688.1
5	150	-688.1
6	180	-708.8
7	210	-708.8
8	240	-708.8
9	270	-708.8
10	300	-708.8
:	:	
45	1350	-711.4
46	1380	-711.4
47	1410	-711.4
48	1440	-711.4
49	1470	-711.4
50	1500	-711.4

The residual stress function during high temperature processes *Tf3* at 650°C and *Tf4* at 850°C is shown in Fig. 6.

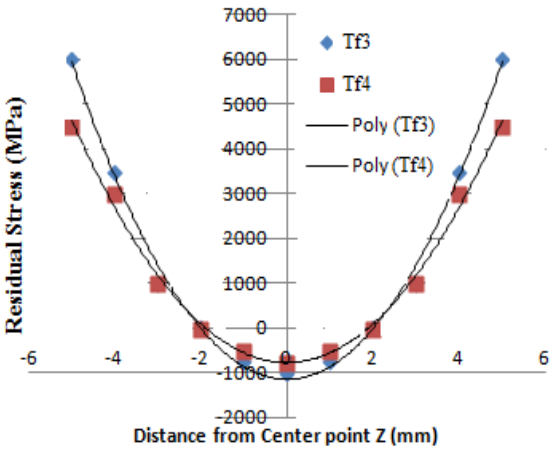

Fig. 6. Residual stress *Tf3* at 650°C and *Tf4* at 850°C.

The optimal residual stresses with GA in high temperature process at 650°C and 850°C are given in Table 3.

Table 3. Optimal Residual Stress in high temperature process with genetic algorithm

Temperature (°C)	Residual Stress $\sigma(z)$ (MPa)	Distance z (mm)
650°C	-711.3689	0.002934
850°C	-969.868	0.002757

The analytical calculation results for residual stress, based on (4), at the positions obtained from the simulation fis given in Table 4.

Table 4. Residual Stress obtained from analytical calculation

Temperature (°C)	Residual Stress $\sigma(z)$ (MPa)	Distance z (mm)
650°C	-975.556	0.002934
850°C	-1061.134	0.002757

The residual residual stress value with GA approach at 650°C is -711.3689 MPa and with analytical calculation is -975.556 MPa. There is a difference of about 27 %. The difference may be caused by various factors. Thus, a better fit may also be obtained by several alternative approaches. For instance, the number of simulation rounds in GA may be increased. Other alternatives involve selecting different values of parameters in GA such as the parameters of the size of population, probability of recombination or crossover (*pc*), and probability of mutation (*pm*). It must be noted that for a particular population size, there is a particular range of *pc* and *pm* values which will result in optimum fitness value for all generations and/or fast simulation times. Generally GA is more efficient than analytical calculations, because with a reasonable number of simulations it can achieve the optimal value of fitness function in certain range. At the temperature of 850°C the residual stress value obtained with GA is -969.868 MPa and with analytical calculation is -1061.134 MPa. This difference is only about 8.67%.

Table 5 presents the residual stress estimated from analytical calculations with (4) for several distances z from the center point. Those are to be used for modeling using FNN.

Table 5. The residual stress based on analytic calculation

z (mm)	$\sigma(z)$
-0.569	-975
-1.106	-711
-2.111	-244
-2.030	-145
-1.900	-6.59
-1.911	6
-2.030	146
-2.051	171
-2.116	250
-2.225	389
-2.455	710
-2.625	965

The result of the grouping or clustering for the distribution of the residual stress using FNN concentration in two-dimension is shown in Fig. 7. The center for residual stress distribution based on (2) and (3) is found as (-76, 76) MPa.

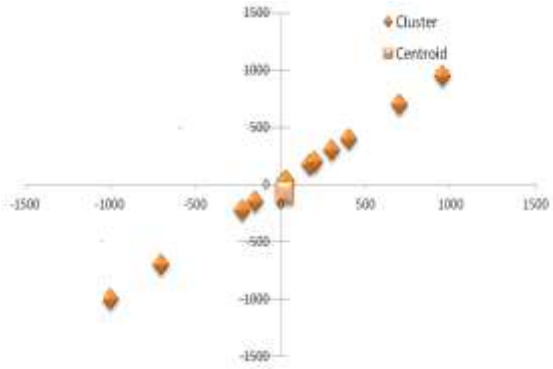

Fig. 7. The center of residual stress distribution.

By using ANN simulation modeling based on (1), the trend of residual stress was obtained for training data. The plot of the data for the trend of the residual stress prediction using ANN is shown in Table 6 and Fig. 8.

Table 6. The residual stresses found from simulation

z (mm)	$\sigma(z)$
-2	330
-1.5	250
-1	50
0	-85
0.5	-90
1.5	-75
1	-40
3	250
4	390

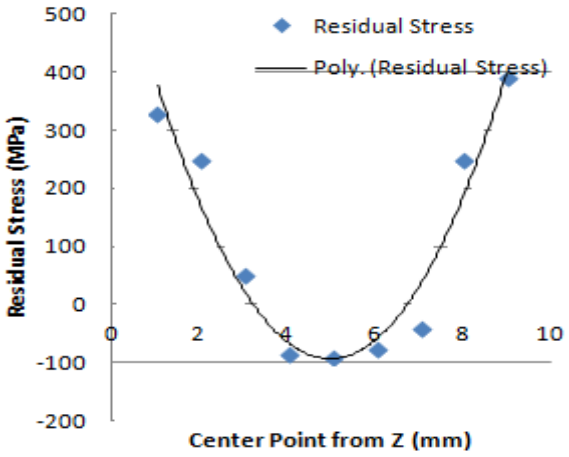

Fig. 8. Residual stress trend determined using ANN.

Figure 9 shows the adjusted residual coefficient (R) of the estimation process simulation modeling in ANN. The adjusted residual coefficient of modeling results is expressed in the parameter R = 0.94397. Since R *is* close to one, it indicates that the results of the estimation are in accordance with the expected modeling. It can be suggested that the model estimated approximates the expected model.

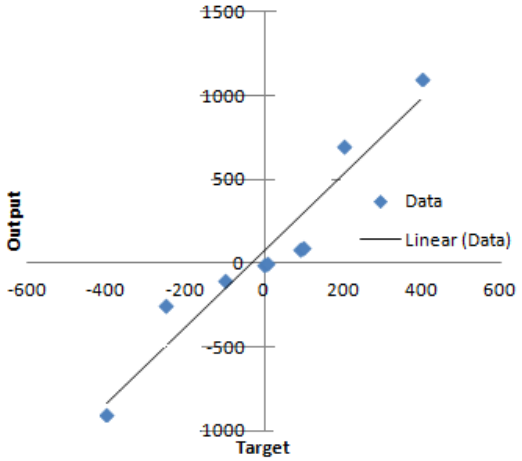

Fig. 9. The results of the estimation process by ANN (R = 0.94397).

The residual stress model is a polynomial degree two with coefficients p_1, p_2 and p_3 whose values and ranges are 50.33 (33.77; 67.28); -76.54 (-121; -32.03) and -55.2 (-133; 22.66), respectively, with an error deviation of 7.874.

CONCLUSION

The optimal parameter values of the GA-based residual stress model for high temperature materials processing were obtained. The minimal residual stress simulations with GA at a final temperature of 650°C converged to the value of -711.3689 MPa at 0.002934 mm from the center point while with analytical calculations resulted in -975.556 MPa. At 850°C, GA simulation results converged to -969.868 MPa while analytical calculations give -1061.13 MPa at 0.002757 mm from the center point. The difference between GA and analytical results for residual stress at the same distance from center point is about 27% at the temperature 650°C and about 8.67% at the temperature of 850°C. The difference may be reduced by increasing the number of simulations in GA or by changing the parameters in GA. GA is more efficient than analytical calculations, because with a reasonable number of simulation it can achieve the optimal value fitness function

for some parameters within a certain range. The measures of central tendency for clustering data using the FNN have coordinates (-76; 76) MPa. While the model with ANN has the polynomial degree two with adjusted coefficient is 0.94397. This value close to one, that means the results of model are quite good. The coefficients of trend residual stress p_1, p_2 and p_3 respectively are 50.33 (33.77; 67.28); -76.54 (-121; -32.03) and -55.2 (-133; 22.66) with an error deviation of 7.874.

REFERENCES

1. J.E. Raja Dhas and S. Kumanan, Indian Journal of Engineering and Material Science **18** (2011) 351.
2. M. Jeyakumar, T. Christopher, R. Narayanan *et al*., Indian Journal of Engineering and Material Science **18** (2011) 425.
3. P. Sathiya, K. Pannerselvam and M.Y. Abdul Jaleel, Material and Design, Elsevier **36** (2012) 490.
4. W. Jiang and K. Yahiaoui, International Journal of Pressure Vessels and Piping, Science Direct, **95** (2012) 39.
5. A.H. Yaghi, TH, Hyde, A.A. Becker *et al*., International Journal of Pressure Vessels and Piping, Science Direct **111-112** (2013) 173.
6. M. Jeyakumar and T. Christopher, Chinese Journal of Aeronautics **26** (2013) 1415.
7. J.E. Raja Dhas and S. Kumanan, Applied Soft Computing **14**, Part C, January (2014) 461.
8. H.X. Yuan, Y.Q. Wang, Y.J. Shi *et al*., Journal Thin-Walled Structures, Elsevier **79** (2014) 38.
9. H. Vemanaboina , S. Alkella and R.K. Buddu, Procedia Materials Science **6** Science Direct (2014) 1539.
10. S. Xu, W. Wang and Y. Chang, Journal International of Pressure Vessels and Piping **119** (2014) 1.
11. P. Dong, S. Song, J. Zhang *et al*., International of Pressure Vessels and Piping **123-124** (2014) 19.
12. M. Islam, A. Buijk, M. Rais-Rohani *et al*., Finite Elements in Analysis and Design **84** (2014) 54.
13. W. Guo, S. Dong, J.A. Francis *et al*., Journal Material Science & Engineering A **625** (2015) 65.
14. M. Gyun Na, J. Weon Kim and D. Hyuk Lim, Nuclear Engineering and Technology **39** (2007) 337.
15. M. Gyun Na, J. Weon Kim, D. Hyuk Lim *et al*., Nuclear Engineering and Design **238** (2008) 1503.
16. X. Zhang and X. Cheng, A. Stelson *et al.,* Journal of Thermal Stresses **25** (2002) 523.